A New Scheme of Force Reflecting Control

Won S. Kim

Jet Propulsion Laboratory
California Institute of Technology
4800 Oak Grove Drive
Pasadena, CA 91109

ABSTRACT

A new scheme of force reflecting control has been developed that incorporates position-error-based force reflection and robot compliance control. The operator is provided with a kinesthetic force feedback which is proportional to the position error between the operator-commanded and the actual position of the robot arm. Robot compliance control, which increases the effective compliance of the robot, is implemented by low pass filtering the outputs of the force/torque sensor mounted on the base of the robot hand and using these signals to alter the operator's position command. This position-error-based force reflection scheme combined with shared compliance control has been implemented successfully to the Advanced Teleoperation system consisting of dissimilar master-slave arms. Stability measurements have demonstrated unprecedentedly high force reflection gains of up to 2 or 3 even though the slave arm is much stiffer than the operator's hand holding the force reflecting hand controller. Peg-in-hole experiments were performed with eight different operating modes to evaluate the new force-reflecting control scheme. Best task performance resulted with this new control scheme.

Introduction

In a typical telemanipulation system that does not support force reflection or compliance control, a stiff remote manipulator moves strictly according to a human operator's position command, and small errors between the actual and the commanded position of the manipulator can give rise to undesired large contact forces and torques. It is thus hard to expect safe and reliable telemanipulation with this system. Two major techniques that alleviate this excessive contact force problem are force reflection [2] and shared compliance control [9]. In force reflecting teleoperation, the operator can feel contact forces and torques through a force reflecting hand controller, and thus adjust the hand controller position naturally to reduce undesired contact force components. Experimental studies indicate a significant enhancement in the human operator's task performance with force reflection [5]. In shared compliant control, the operator's commanded position is altered by a compliant control force feedback in the robot side. This local autonomous force feedback in the robot side adds active compliance and damping to the stiff robot hand, making the robot more compliant to the environment and softening mechanical contacts/collisions between the manipulator and objects. Recent experiments demonstrated that shared compliant control is essential in time-delayed telemanipulation [9].

Recently orbital replacement unit (ORU) changeout experiments were performed with the JPL/NASA telerobot testbed system [7], and the experimental results showed that without shared compliant control (SCC) or force reflection (FR), the operator could not complete the task, while with SCC or FR the operator could perform the task successfully with reduced contact forces both in magnitude and duration. The results also indicated that the task performance with SCC was superior to that with FR in terms of task completion time, cumulative contact force, and total contact duration. The relatively poor performance with FR was mainly due to a poor force reflection gain. The maximum force reflection gain attainable without causing instability was only approximately 1/10. With this low gain, the operator could feel only 1 lb when the manipulator hand senses a 10 lb contact force. It is shown in this paper that the problem of poor force reflection is not specific to this system, but rather inherent to the conventional force reflection control scheme being used for dissimilar master-slave systems where the slave system usually has much higher stiffness than the effective stiffness of the human hand holding the force reflecting hand controller.

A major advantage of FR is that the operator actually feels the contact forces/torques sensed by the telerobot hand. This paper addresses two important issues related to FR: i) a new scheme of force reflecting control that makes high force reflection possible, and ii) assessment of the performance enhancement by providing the operator with both FR and SCC. Recently we developed a new scheme of force reflecting control that enables a sufficiently high force

reflection gain (up to 2 or 3) by utilizing position error and active compliance. This new scheme of FR combined with SCC is described in this paper. We also performed peg-in-hole experiments with eight different operating modes to evaluate this newly developed control scheme, and the results are presented.

Implementation of Position-Error-Based Force Reflection

In a typical force-reflecting telemanipulation system consisting of dissimilar master-slave arms, the position of a slave arm (remote manipulator) is controlled by the human operator through a master arm (force-reflecting hand controller) (Fig. 1), while the contact forces/torques sensed by the force/torque sensor at the base of the robot hand are reflected back to a human operator through the master arm. This forms a closed-loop system, and raises a stability issue. Our experience with the existing force-reflecting systems supporting dissimilar master-slave arms [7],[9] has shown that the force reflection gain from the robot hand to the force reflecting hand controller is limited to approximately 1/10. Namely, the operator can feel only 1 lb when the robot hand senses 10 lb. We now investigate this poor force reflection problem.

As a first-cut rough approximation, we assume a linear decoupled system model in cartesian axis. In Fig. 1, the open-loop transfer function Q(s) is given by

$$Q(s) = G_{ps}G_{fr}K_{me}H(s)R(s), \tag{1}$$

where G_{ps} is the position command scale factor, G_{fr} is the force reflection gain, and K_{me} is the effective stiffness which is a parallel combination of the manipulator stiffness and the environment stiffness. $R(s)$ is the robot servo system transfer function in cartesian space [6],[8] and is given by a linear sum of the six second-order joint servo transfer functions with the DC gain of $R(0)=1$. $R(s)$ could be second-order, forth-order, or higher depending upon the cartesian axis and the arm configuration. An example of a cartesian space frequency response [8] of the PUMA arm used in our Advanced Teleoperation system [2] is shown in Fig. 2. In this example, the double-pole corner frequencies are at about 3 and 6 Hz, behaving as a fourth order system. $H(s)$ is the transfer function of the operator's hand holding the 6-degree-of-freedom force-reflecting hand controller [1]. The transfer function can be obtained by measuring the magnitude ratio of the hand controller deflection to the applied force input for different frequencies. Measurements indicate that the compliance value C_h $(=H(0))$ varies from about 1.0–2.0 in/lb (0.5–1.0 lb/in stiffness) with a loose grasp to about 0.1–0.2 in/lb (5–10 lb/in stiffness) for a firm grasp. The bandwidth of $H(s)$ is about 1 Hz for a loose grasp, and 3 Hz for a firm grasp. Typical frequency responses of the operator's hand holding the force reflecting hand controller for firm grasp (circle) and for loose grasp (triangle) are shown in Fig. 3 In order to have a stable teleoperation system with a constant force reflection gain G_{fr}, the open-loop DC gain $Q(0)$ should not be much greater than 1, since a higher loop gain causes instability due to the higher order
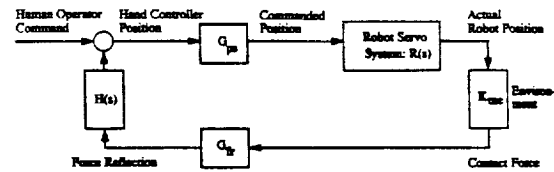

Fig. 1. A typical force-reflecting scheme for dissimilar master-slave arms.
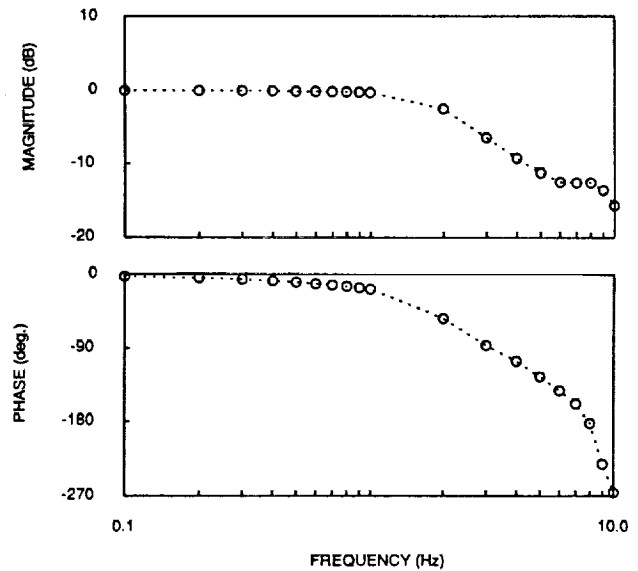

Fig. 2. A typical cartesian space frequency response of the PUMA arm used in our Advanced Teleoperation System
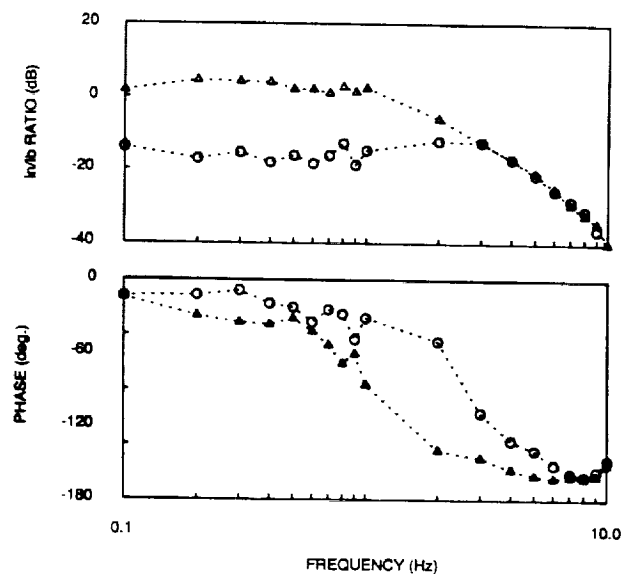

Fig. 3. Typical frequency responses of an operator's hand holding a 6-axis force-reflecting hand controller for firm grasp (circle) and for loose grasp (triangle). The magnitude ratio of the hand controller deflection to the applied force is plotted as a function of frequency.

255

dynamics of $H(s)R(s)$. Namely,

$$G_{fr} \le \frac{1}{G_{ps}K_{me}C_h}. \qquad (2)$$

In our typical system, the combined stiffness of the manipulator and environment is measured $K_{me} = 25\ lb/in$, and we assume that the operator's hand can maintain at least a $2.5\ lb/in$ stiffness $(C_h = 0.4\ in/lb)$ during teleoperation. In this typical situation, the manipulator/environment stiffness is much higher than the operator's-hand/hand-controller stiffness $(K_{me}C_h=10)$, and from (2) the maximum force reflection gain G_{fr} is limited to only $1/10$ for the unity position scaling factor $(G_{ps}=1)$. Our foregoing analysis clearly indicates that the poor force reflection is not due to a poor implementation of the specific systems, but rather inherent to the existing conventional force-reflection system with dissimilar master-slave arms. A good direction to increase the force reflection gain is to make the robot more compliant by employing compliant control.

Shared compliance control has been implemented recently [9] by low pass filtering the outputs of the force/torque sensor mounted on the base of the robot and using these signals to alter the human operator's position/orientation command (Fig. 4). This low-pass-filtered force/torque feedback has an effect of giving the robot hand behavior similar to a damped spring (in each of the task space dimensions) in series with the stiff, position-controlled, robot manipulator. An approximate mechanical equivalent of the above implementation consists of a spring connected in parallel with a damper. It can be shown that the compliance control force feedback gain G_{cc} is approximately the new compliance value of the manipulator system in Fig. 4.

We now consider a simple combination of FR with SCC as shown in Fig. 5. This combination results in a system having two feedback loops; the inner compliance control loop residing in the robot side, and the outer force reflection loop with the operator in the loop. At first glance, one might think from (2) that the simple combination of SCC and FR of Fig. 5 should increase the force reflection gain markedly, since the inner compliance control loop makes the manipulator/environment stiffness K_{me} very low, approximately $1/G_{cc}$. Experimental testings however revealed that this simple combination increases the maximum force reflection gain only slightly. This can be understood by noting that the compliant control has a low pass filter whose bandwidth is lower than the manipulator bandwidth. As the frequency increases above the low pass filter bandwidth, the effect of the inner compliant control loop diminishes resulting in the original model of Fig. 1, and thus in this scheme SCC does not contribute much to improve the force reflection gain.

An alternate way of providing FR is to utilize the position error between the commanded and the actual position of the robot arm. Namely, we can have force reflection proportional to the position error Δx, namely $f_{hc} = G_{pe}\Delta x$. Although this position-error-based force reflection technique has been widely used in replica master-slave arms as a standard approach to achieve the unity force reflection gain, its
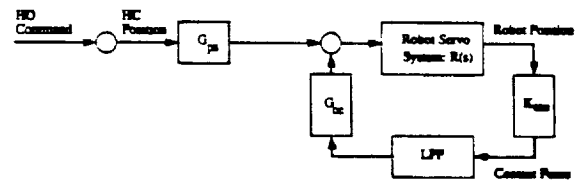

Fig. 4. Shared compliance control implementation with low-pass-filtered force/torque feedback.
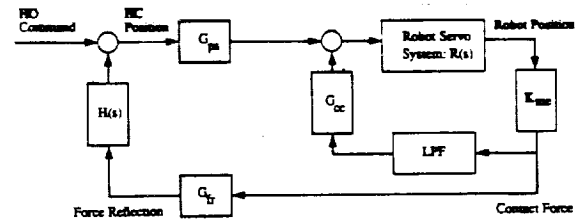

Fig. 5. A simple combination of force reflection with shared compliance control. This scheme does not increase the force reflection gain noticeably.
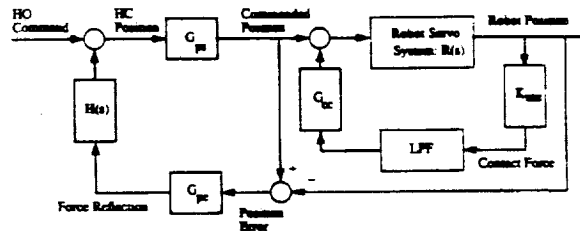

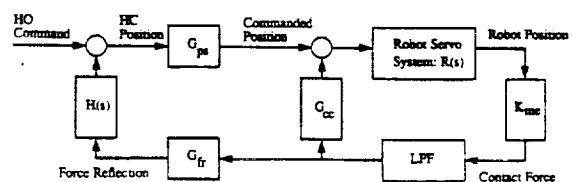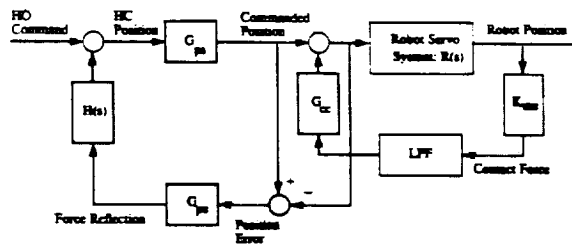Fig. 6. Position-error-based force reflection with compliance control.

Fig. 7. A variation of the position-error-based force reflection with compliance control (a) and its equivalent conversion resulting in low-pass-filtered force reflection with compliance control (b).

256

implementation to dissimilar master-slave arms resulted in poor force reflection, since the slave arm is usually much stiffer than the operator's hand holding the hand controller (master arm). We have recently succeeded in developing a new scheme of force reflecting control that enables the system to have a sufficiently high force reflection gain (up to 2 or 3) for dissimilar master-slave arms by combining the position-error-based force reflection with compliance control (Fig. 6). Compliance control is essential to achieve high force reflection gain. In this scheme the force reflection gain is given by $G_{pe}G_{cc}$, since the contact force f_{rh} at the robot hand deflects the hand by $\Delta x = G_{cc}\,f_{rh}$, and the drive force of the force reflecting hand controller is then related to the robot contact force by $f_{hc} = G_{pe}\Delta x = G_{pe}G_{cc}\,f_{rh}$. It is interesting to observe that in this scheme the force/torque sensor outputs are not directly used for force reflection. Instead, the force/torque sensor outputs are used for robot compliance control, while the position/orientation errors which are generated in proportion to robot compliances are used for force reflection.

A variation of the position-error-based force reflection has eventually led to an alternate scheme that also enabled the system to have high force reflection. By noting that the robot servo system cartesian-space transfer function for each cartesian axis is close to 1 for low frequencies ($R(0)=1$), the control scheme of Fig. 6 is slightly changed as shown in Fig. 7a, which can then be equivalently converted to Fig. 7b with $G_{fr} = G_{pe}G_{cc}$. This resulted in another new scheme of force reflecting control. In this scheme, low-pass-filtered contact forces, instead of pure uncompensated forces, are fed back to the operator. Note that a simple idea of combining pure force reflection and compliance control of Fig. 5 did not allow high force reflection, while this new scheme enables the system to have high force reflection (up to 2 or 3) by using low-pass-filtered force reflection, instead of uncompensated pure constant gain force reflection, is used in combination with compliance control. The above two newly developed schemes --- position-error-based force reflection with compliance and low-pass-filtered force reflection with compliance --- appear to be similar in characteristics and performance. In both schemes, high force-reflection is achieved only with a limited bandwidth that is the same bandwidth imposed by the low pass filter of the compliance control compensator. An interesting feature observed in the position-error-based force reflection is that the operator feels artificial force when the operator moves the hand controller faster than the actual robot motion.

Compliance, Force Reflection, and Stability Measurements

In order to characterize the force reflection and compliance behavior of the system, the force-input/digital-output characteristic of the force/torque sensor [3] and the digital-input/force-output characteristic of the force reflecting hand controller [1] were roughly measured manually by using a force gage. Measurements indicate that the force/torque sensor reading is fairly linear up to ± 10 *lb* for the x, y, z translations (Fig. 8, upper panel) and ±12 *lb·in* for the roll,
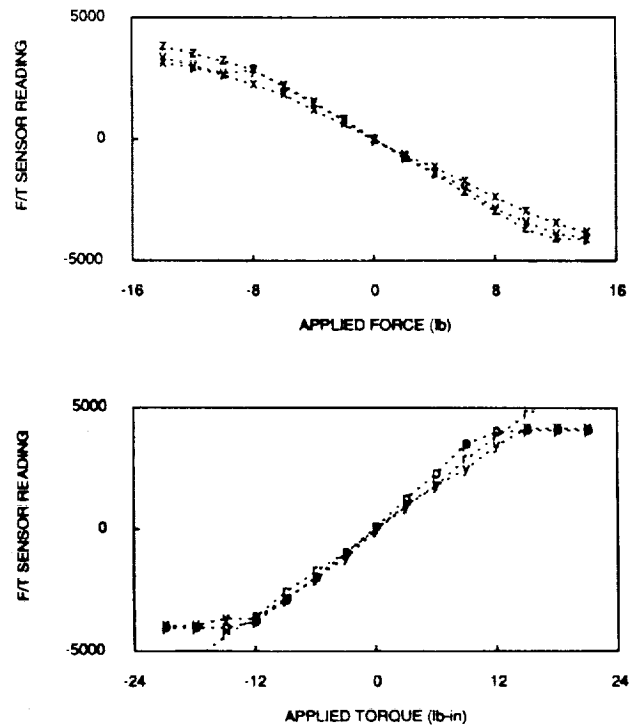

Fig. 8. Digital readout vs. applied input force/torque measurements of the force/torque sensor for x, y, z translations (upper) and for roll, pitch, yaw rotations (lower).
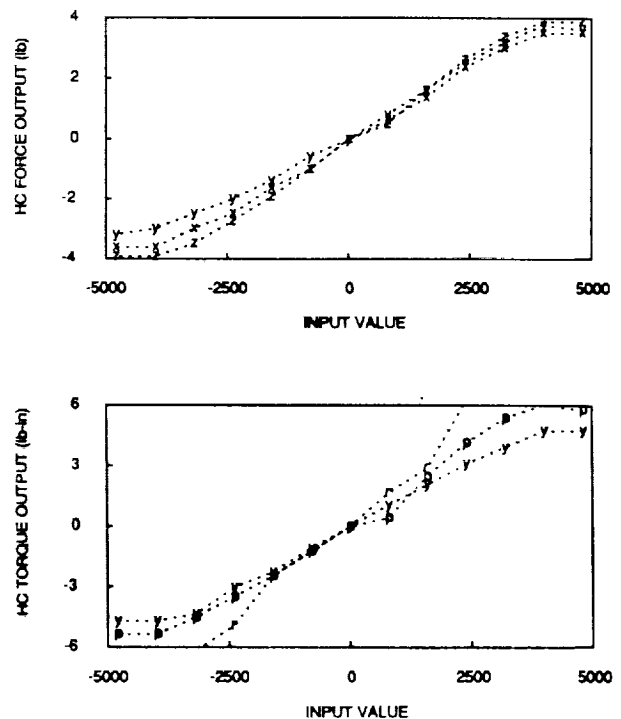

Fig. 9. Force/torque output vs. digital input measurements of the force reflecting hand controller for x, y, z translations (upper) and for roll, pitch, yaw rotations (lower).

257

pitch, yaw rotations (Fig. 8, lower). The force/torque drive behavior of the force reflecting hand controller is fairly linear up to about ±4 *lb* (Fig. 9, upper) for translations and about ±4 *lb·in* for rotations (Fig. 9, lower).

Compliance measurements (robot hand deflection vs. applied force) of SCC of Fig. 4 were plotted in Fig. 10 for four compliance feedback gains, G_{cc} = 1/16, 1/8, 1/4, and 1/2 *in/lb*. The plots show that the new compliance value of the robot hand is approximately equal to the compliance compensator feedback gain G_{cc}. The measured compliance data also show excellent linearity in the robot work volume. In the SCC implementation, a low pass filter is used to add damping to stabilize the system. A larger compliance means a higher compliance feedback gain (G_{cc}), which requires a lower bandwidth of the low pass filter with a more sluggish compliant response. The maximum bandwidths of the low pass filter for given desired compli-
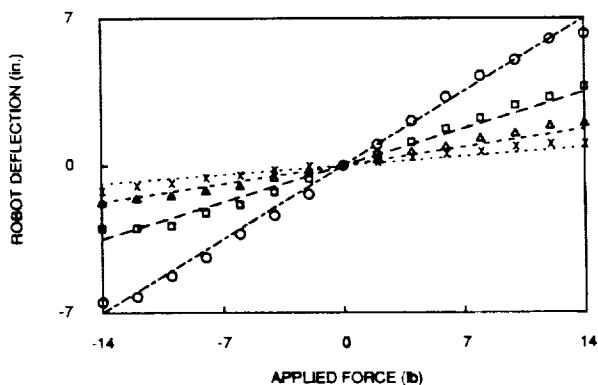

Fig. 10. Compliance measurements of the shared compliance control: robot hand position deflection vs. applied force to the robot hand for four compliance compensator feedback gains of G_{cc} = 1/16 (x), 1/8 (triangle), 1/4 (square) and 1/2 (circle) *in/lb*.
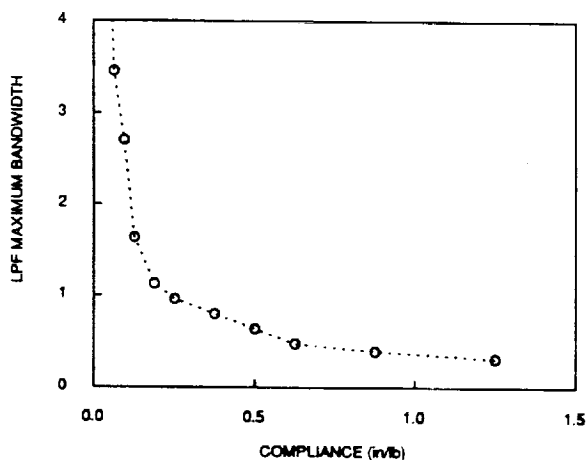

Fig. 11. Maximum bandwidth of the low pass filter vs. compliance value (compliance compensator feedback gain) measurements for the shared compliance control of Fig. 4.

ance values were measured and plotted in Fig. 11. The maximum bandwidth of the low pass filter is about 3.4 *Hz* for the compliance value of G_{cc} = 1/16 *in/lb* (16 *lb/in* stiffness), 1.6 *Hz* for 1/8 *in/lb*, 0.8 *Hz* for 1/4 *in/lb*, and 0.4 *Hz* for 1/2 *in/lb*. In the above measurements, compliance compensators were added only along translational axes not about rotational axes. When both were enabled, the maximum bandwidth values were reduced further approximately to a half. A more detailed stability analysis can be found in [6].

The force reflection behaviors of the position-error-based force reflection scheme of Fig. 6 were measured (Fig. 12) for the three force reflection gains of 1/4 $(G_{cc}$ = 1/16 *in/lb*), 1/2 $(G_{cc}$ = 1/8 *in/lb*), and 1 $(G_{cc}$ = 1/4 *in/lb*) with a fixed position error gain of G_{pe} = 4 *lb/in*. Note that the force reflection gain in this scheme is given by $G_{pe}G_{cc}$. In Fig. 12, all three curves saturate at about 4 *lb* drive force, since the maximum drive force of the force reflecting hand controller is limited to about 4 *lb* as shown in Fig. 9. This limited drive force is probably a good feature since excessive force in the hand controller causes rapid operator fatigue.

Fig. 13 is a plot showing the maximum bandwidth vs. the force reflection gain for the position-error-based force reflection with three different compliance values of the compliance compensator $(G_{cc}$ = 1/16, 1/8, 1/4 *in/lb*). For a given compliance value, both the bandwidth and the force reflection gain are limited. It is interesting to observe that an abrupt oscillation occurs as soon as the force reflection gain exceeds a certain maximum value. In Fig. 13, the maximum bandwidths for the compensator compliance values of 1/16, 1/8, 1/4 *in/lb* are 3.4 *Hz*, 1.6 *Hz*, 0.8 *Hz*, respectively, and the maximum force reflection gains for the same compliance values are 0.375, 0.75, 1.5, respectively. These data indicate that the maximum bandwidth is inversely proportional to the compliance value, while the maximum force reflection gain is proportional to the compliance value. The maximum bandwidths are limited by the stability boundary of the compliance control feedback loop as described earlier (Fig. 11). The maximum force reflection gains are somewhat higher than expected from (2), and a more careful stability analysis is in progress.
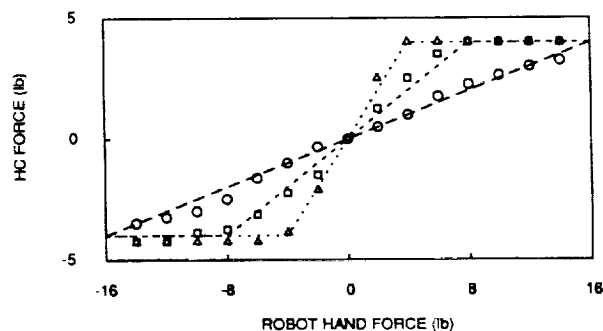

Fig. 12. Force reflection characteristics of the position-error-based force reflection combined with compliance control for the force reflection gains of 1/4 (circle), 1/2 (square), and 1 (triangle).

258

The maximum force reflection gains of the position-error-based force reflection with four different position scale factors (G_{ps} = 1/4, 1/2, 3/4, 1) were measured and plotted in Fig. 14 for four different compliance values of the compliance compensator (G_{cc} = 0, 1/16, 1/8, 1/4 in/lb). The maximum force reflection gain is inversely proportional to the position scale factor G_{ps}, which can be easily conjectured from (2). We can observe in Fig. 14 that the maximum force reflection gains are approximately doubled when the position scale factor is doubled, for example, from 1/2 to 1. The position-error-based force reflection is possible without compliance control (G_{cc}=0) as seen in Fig. 14, but the maximum force reflection gain is limited to about 1/10 for the unity position scale factor.
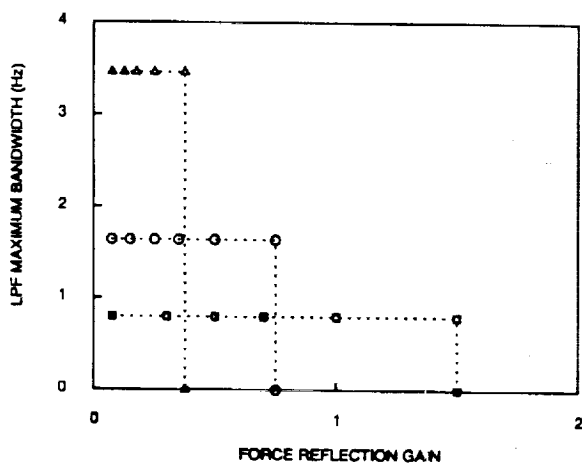

Fig. 13. Maximum bandwidth of the low pass filter vs. force reflection gain measurements of the position-error-based force reflection with compliance control for three compliance values of 1/16 (triangle), 1/8 (circle), and 1/4 (square) in/lb.
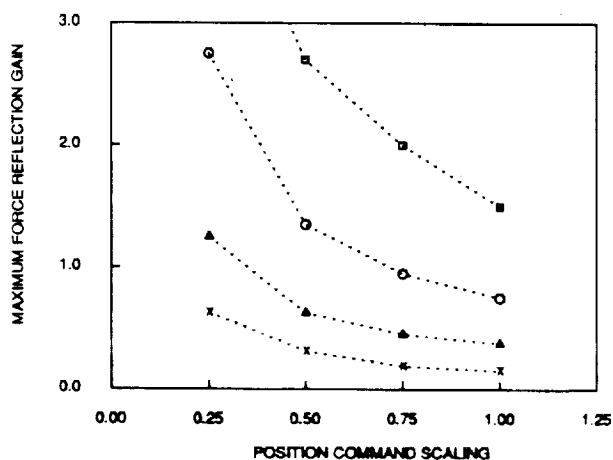

Fig. 14. Maximum force reflection gain vs. position scale factor measurements of the position-error-based force reflection with compliance control for four compliance values of 0 (x), 1/16 (triangle), 1/8 (circle), and 1/4 (square) in/lb.

Peg-in-Hole Experiments with Different Operating Modes

Peg-in-hole tasks were performed with eight different operating modes to evaluate the position-error-based force reflection in comparison with other operating modes. A 7"x7" peg-in-hole task module mounted on the 21"x21" task board [5] was used for the peg-in-hole task. The peg-in-hole task module has 9 holes arranged in a square matrix. In our experiments, only one hole with 10 mil clearance and no chamfer was used. The peg was 4.75" in length and 0.998" in diameter. The peg-in-hole task consisted of the following steps: i) the peg is initially located at about 2 inches in front of the designated hole of the peg-in-hole task module, ii) move the peg to the designated hole, iii) insert the peg into the hole completely, iv) extract the peg. In our Advanced Teleoperation setup, the hand controller of the master side was installed in the control station room separate from the PUMA arm of the slave side. Three television camera views of the task board and robots were provided in the control station: top, upper left, and upper right views of the task environment. The focus and zoom settings were fixed throughout the experiments. During the experiments, force/torque data of the robot hand were recorded to a hard disk at 100 Hz sampling rate through a parallel I/O port of an IBM computer.

The eight operating modes tested are: (mode 1) low-pass-filtered FR combined with SCC with the FR gain = 1/2, (mode 2) position-error-based FR combined with SCC with the FR gain = 1/2, (mode 3) low-pass-filtered FR combined with SCC with the FR gain = 1/4, (mode 4) SCC only, (mode 5) damper only control with no active compliance, (mode 6) uncompensated pure FR with the FR gain = 1/10, (mode 7) pure position control without FR or SCC, and (mode 8) rate control with SCC. For all position control modes of 1 through 7, the position scale factor is fixed to G_{ps}=1/2. The stiffness values (inverse of the compliance values) used for SCC were 6.7 lb/in (80.0 lb/ft) for cartesian translations and 2.8 $lb \cdot in/deg$ (13.4 $lb \cdot ft/rad$) for cartesian rotations. The low pass filter bandwidths were 0.63 Hz for translations and 0.47 Hz for rotations. For simplicity, the same compliance and bandwidth values were used for all three cartesian position axes, and so were for all three orientation axes, and no serious attempt was made to find the optimal parameter values.

In the experiments, test operators performed the peg-in-hole task three times each with the 8 operating modes in random order (24 tasks in total). Three test operators participated in the experiments. All operators first trained themselves until they could complete the peg-in-hole task comfortably for all operating modes. Then, each operator performed one complete set of the experiment of 24 peg-in-hole tasks as a practice run. Thereafter, actual experiment was performed for experimental data collection.

Task completion times and cumulative contact forces were computed from the contact force/torque data recorded during the experiment and the means and standard deviations of the three test operators' data are plotted in Fig. 15. From Fig. 15, we can observe that completion times are similar for all position control modes, but contact forces are

greatly reduced with the use of SCC and/or FR. Performance with position control (modes 1 through 7) is superior to that with rate control. The best task performances resulted with our newly developed schemes --- position-error-based FR with SCC and low-pass-filtered FR with SCC. Both schemes combine FR and SCC, and enable high force reflection with limited bandwidths. Due to limited bandwidth, operators felt force reflection sluggishness during the peg-in-hole task execution. Some operators felt more comfortable with a reduced force reflection gain of 1/4 compared to 1/2, although the task performance was better with the force reflection gain of 1/2 in terms of cumulative contact force as shown in Fig. 15. Performance with SCC only or damper only was superior to that with uncompensated pure force reflection (force reflection gain = 1/10) as seen in Fig. 15, which agree with previous experiments [7]. Low-pass-filtered FR alone without SCC was marginally

operational, requiring the operator to maintain a very firm grasp during the peg-in-hole task performance, and thus was not included in our experiment.

Recently more thorough experiments with a screw insertion/removal task [4] were performed with seven test operators to compare various control modes. Again the newly developed position-error-based force reflection combined with compliance control resulted in the best task performance among all control modes tested.

Conclusion

A new scheme of force reflecting control --- position-error-based force reflection combined with compliance control --- has been developed for dissimilar master-slave arms. This new scheme has enabled the system to have high force reflection gain (up to 2 or 3), which was not possible with a conventional scheme when the slave arm is much stiffer than the master arm. The experimental results with a peg-in-hole task indicate that the newly developed position-error-based force reflection combined with compliance control resulted in best task performance.
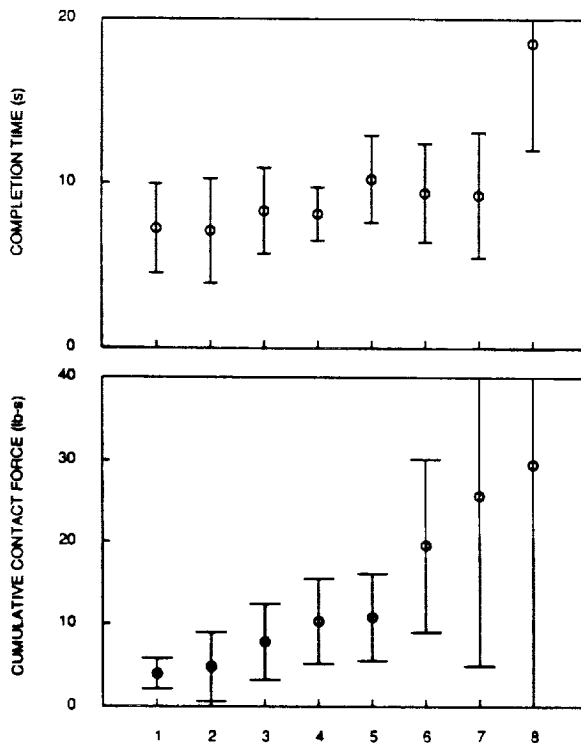
Fig. 15. Completion time (a) and cumulative contact force (b) plots for the peg-in-hole task (1-inch-diameter peg with 10-mil clearance) with 8 different operating modes. Means (circles) and standard deviations of three test operators' data are plotted. Mode 1: low-pass-filtered force reflection (FR gain = 1/2) with compliance, Mode 2: position-error-based force reflection (FR gain = 1/2) with compliance, Mode 3: low-pass-filtered force reflection (FR gain = 1/4) with compliance, Mode 4: shared compliance control only (compliance and damper), Mode 5: damper only, Mode 6: pure uncompensated force reflection only (FR gain = 1/10), Mode 7: pure position control, and Mode 8: rate control with compliance.

References

[1] A. K. Bejczy and J. K. Salisbury, "Kinesthetic Coupling Between Operator and Remote Manipulator," Proceedings: ASME International Computer Technology Conference, vol. 1, pp. 197-211, San Francisco, CA, Aug. 1980.

[2] A. K. Bejczy, Z. Szakaly, and W. S. Kim, "A Laboratory Breadboard System for Dual-Arm Teleoperation," Third Annual Workshop on Space Operations Automation and Robotics (SOAR '89), pp. 649-660, NASA Johnson Space Center, TX, July, 1989.

[3] A.K. Bejczy, Z. Szakaly, and T. Ohm, "Impact of End Effector Technology on Telemanipulation Performance," Third Int. Workshop on Space Operations Automation and Robotics (SOAR '89), pp. 429-440, NASA Johnson Space Center, Houston, TX, July 1989.

[4] H. Das, H. Zak, W. S. Kim, A. K. Bejczy, and P. Schenker, "Performance Experiments with Alternative Advanced Teleoperator Control Modes for a Simulated Solar Max Satellite Repair," Fifth Annual Workshop on Space Operations, Applications, and Research Symposium (SOAR '91), NASA Johnson Space Center, TX, July, 1991.

[5] B. Hannaford, L. Wood, B. Guggisberg, D. McAffee, H. Zak, "Performance Evaluation of a Six-Axis Generalized Force-Reflecting Teleoperator," JPL Publication 89-18, June 1989.

[6] W. S. Kim, "Shared Compliant Control: a Stability Analysis and Experiments," IEEE Conf. on Systems, Man, and Cybernetics, pp. 620-623, Los Angeles, CA, Nov. 1990.

[7] W. S. Kim, P. G. Backes, S. Hayati, and E. Bokor, "Orbital Replacement Unit Changeout Experiments with a Telerobot Testbed System," IEEE Int. Conf. on Robotics and Automation, pp. 2026-2031, Sacramento, CA, April 1991.

[8] W. S. Kim and A. K. Bejczy, "A Stability Analysis of Shared Compliance Control," Japan-USA Symposium on Flexible Automation, pp. 567-572, Kyoto, Japan, July 1990.

[9] W. S. Kim, B. Hannaford, and A. K. Bejczy, "Shared Compliance Control for Time-Delayed Telemanipulation," First Int. Symposium on Measurement and Control in Robotics, NASA Johnson Space Center, Houston, TX, June 1990.